Thermochimica Acta 491 (2009) 5–9

Contents lists available at ScienceDirect

Thermochimica Acta

journal homepage: www.elsevier.com/locate/tca

Structural and thermal transport properties of Zn_xTe_{100-x} (x = 5, 10, 30 and 50) alloys

V. Kishore[a,b,*], V.K. Saraswat[a,b], R. Sharma[a], N.S. Saxena[a], K.B. Sharma[a], T.P. Sharma[a]

[a] Semiconductor and Polymer Science Laboratory, Department of Physics, University of Rajasthan, 5-6, Vigyan Bhawan, Jaipur-302 004, India
[b] Dept. of Physics, Banasthali University, Banasthali 304022, Tonk, Rajasthan, India

ARTICLE INFO

Article history:
Received 4 October 2008
Received in revised form 13 February 2009
Accepted 15 February 2009
Available online 28 February 2009

PACS:
61.10.–I
81.70.P

Keywords:
Thermal conductivity
Thermal diffusivity
Specific heat

ABSTRACT

Measurements of effective thermal conductivity (λ_e) and effective thermal diffusivity (χ_e) of twin pellets of Zn_xTe_{100-x} (x = 5, 10, 30 and 50) chalcogenide materials, prepared under load of 5 tons (equivalent pressure ≈433 MPa) have been made simultaneously at room temperature using transient plane source (TPS) technique. Specific heat per unit volume (C_p) has also been determined from the so obtained data of λ_e and χ_e. The material has been prepared by melt quenching method. The results indicate that both the values of λ_e and χ_e increase logarithmically with increasing Zn concentration. This behaviour of λ_e and χ_e with zinc concentration can be explained by change of bond formation from covalent to ionic in this system. An effort has also been made to predict these values by an empirical relation. X-ray diffraction (XRD) studies for structural investigation of ZnTe have also been carried out and found to be polycrystalline in nature.

1. Introduction

Great attention has been given to II–VI group chalcogenide materials, in recent years, mainly due to their wide range applications as solid-state devices both in scientific and technological field [1]. These materials have come under increased scrutiny because of their wide use in cost reduction of devices for photovoltaic applications [2]. The research on renewable energies includes the photovoltaic conversion of solar energy and important investigations of novel materials and structures [3]. Among II–VI semiconductors, ZnTe and CdTe, are materials of special technological interest. ZnTe is used as a substrate for the growth of CdTe. Heterostructures based on ZnTe and HgTe are used for infrared optics. When doped with vanadium, ZnTe becomes a photo refractive semi conducting material. This has potential applications for optical power limiting. Also ZnTe has been investigated for its uses as visible light-emitting semiconductor laser [4].

In recent years there has been a growing interest in the study of ZnTe material, as it is a potentially low cost semiconductor for switching devices and multi-junction solar cells. ZnTe, being a wide and direct band gap (2.26 eV) semi conducting material with low electronic affinity (3.53 eV), can absorb photons in the visible region without any phonon assisted mechanism that makes it useful in several electro-optic and opto-electronic applications. Recent advancements in thin film solar cell technology have indicated that ZnTe and its alloys may effectively been used in CdTe-based solar cells. Polycrystalline ZnTe material and its alloys like CdZnTe were successfully utilized in the fabrication of tandem solar cell structures with a tailored band gap and quantum well structures. ZnTe was also proposed as passivation layer for HgTeCd surfaces for metal–insulator–semiconductor (MIS) devices. All these created a renewed interest in the studies of ZnTe material for the fabrication of devices [5]. The use of ZnTe in these fields needs that the alloy should be synthesized inexpensively and suitable for industrial applications. In order to make use of this technique in industrial applications, a better understanding of their physical mechanisms is desirable. The knowledge of thermal transport properties of a material in bulk form has useful significance from structural point of view. Thermal transport properties like thermal conductivity, thermal diffusivity and specific heat of these materials are influenced by the scattering of phonons with crystal defects, impurities and dislocations present in them. Attempts have been made from time to time to investigate the thermal transport properties of loose granular materials, insulating building material, composites, plastics [6], chalcogenide glasses [7] and polymers [8] using transient methods. Nevertheless, very few efforts have been made to understand the heat energy dissipation through polycrystalline materials.

* Corresponding author at: Semiconductor and Polymer Science Laboratory, Department of Physics, University of Rajasthan, 5-6, Vigyan Bhawan, Jaipur-302 004, India.
E-mail addresses: Kishore_vimal@sify.com (V. Kishore), n.s.saxena@rediffmail.com (N.S. Saxena).

0040-6031/$ – see front matter © 2009 Elsevier B.V. All rights reserved.
doi:10.1016/j.tca.2009.02.014

Thermal conductivity investigations yield useful information on several properties of the material. Studies of the variation of effective thermal conductivity (λ_e) and effective thermal diffusivity (χ_e) of ZnTe at different Zn concentration provides a deeper insight into the nature of the vibrational modes of the crystal lattice and various scattering processes that serve to limit the mean free path of heat carriers, i.e. phonons and electrons (holes) [9].

In the present work, an investigation has been undertaken to study the variation of λ_e and χ_e of Zn_xTe_{100-x} (x = 5, 10, 30, and 50) system using TPS technique. Specific heat per unit volume (C_p) has also been determined using the acquired data on λ_e and χ_e. A comparative XRD study for structural investigation of ZnTe has also been carried out to know clearly about structural changes that occur with different Zn concentrations.

2. Transient Plane Source (TPS) theory

Transient plane source (TPS) technique [10] has been used to carry out measurements of effective thermal conductivity (λ_e) and effective thermal diffusivity (χ_e). Specific heat per unit volume (C_p) has been derived from λ_e and χ_e. The sample which are in the form of pellets of 12 mm diameter and 2 mm thickness and the surfaces of these pellets are smooth so as to ensure perfect thermal contact between the samples and the heating element, as the TPS sensor is placed in between the two pellets of sample material in the sample holder.

The change in the voltage was recorded with a digital voltmeter, which was on line to the personal computer. The power out put to sample was adjusted according to the nature of the sample material and was in the range of 6×10^{-6}–16×10^{-6} W/m^2.

The measurements reported in this paper were performed with a TPS element. It is made of a 10 μm thick nickel foil with an insulating layer made of 50 μm thick Kapton, on each side of the metal pattern. Evaluation of these measurements was performed in a way mentioned by Gustafsson et al. [11]. In experiments with insulating layers of such thickness, it is necessary to ignore the voltage recorded during the first few seconds because of the influence of the insulating layers. However, due to the size of the heated area of the TPS elements, the characteristic time of the experiment is so long that, it is possible to ignore a few seconds of recorded potential difference values and still obtain very good result.

An important aspect of the design of any TPS element is that the pattern should be such that as large a part of "hot" area as possible should be covered by the electrically conducting pattern, as long as there is insulation between the different parts of the pattern. This is particularly important when insulating layers are covering the conduction pattern and the surface (s) of the sample. It should be noted that the temperature difference across the insulating layer could be considered constant after a short initial transient.

3. Experimental details

3.1. Material preparation

Zn_xTe_{100-x} alloys were made by using melt-quenching method. High purity (99.99%) tellurium granules and fine Zn dust in appropriate atomic percentage were weighed in a quartz glass ampoule (length 5 cm and internal diameter 8 mm). The content of the ampoule was sealed in a vacuum of 10^{-6} Torr and heated in a furnace where temperature was raised at a rate of 3–4 K/min up to 1070 K and kept around at that temperature for 10 h. The ampoules were frequently rocked to ensure the homogeneity of the melt. The molten samples were then rapidly quenched in ice-cooled water. Then pellets of thickness 2 mm and diameter 12 mm were prepared by a pressure machine from the powder of the ingot samples. The pellets were made at a constant load of 5 tons (equivalent pressure ≈4.33×10^8 Pa).

Table 1
X-ray diffraction data of $Zn_{10}Te_{90}$ material.

2θ	sin θ	d (Å)	d* (Å)	Plane (h k l)	Identification
32	0.2755	3.52	3.52	111	ZnTe
35	0.3006	3.22	3.23	101	Te
48.8	0.4129	2.35	2.35	102	Te
51.6	0.4350	2.23	2.23	110	Te
53.4	0.4491	2.16	2.16	220	ZnTe
55.4	0.4646	2.09	2.09	111	Te
57.2	0.4785	2.02	2.00	006, 105	Te
58.8	0.4907	1.97	1.98	003	Te
63.6	0.5267	1.84	1.84	311	ZnTe
65.8	0.5429	1.78	1.78	112	Te
73.6	0.5988	1.62	6.62	202	Te
82	0.6557	1.48	1.48	113	Te
83.2	0.6637	1.46	1.46	210	Te

Table 2
X-ray diffraction data of $Zn_{30}Te_{70}$ material.

2θ	sin θ	d (Å)	d* (Å)	Plane (h k l)	Identification
32	0.2755	3.52	3.52	111	ZnTe
35	0.3006	3.22	3.23	101	Te
37	0.3171	3.05	3.05	200	ZnTe
48.2	0.4081	2.37	2.36	220	Te
48.8	0.4129	2.35	2.35	102	Te
51.6	0.4350	2.23	2.23	110	Te
53.4	0.4491	2.16	2.17	220	ZnTe
55.4	0.4646	2.08	2.09	111	Te
57.2	0.4785	2.02	2.00	006, 105	Te
58.8	0.4907	1.97	1.98	003	Te
63.6	0.5267	1.84	1.84	311	ZnTe
65.8	0.5429	1.78	1.78	112	Te
66.8	0.5502	1.76	1.76	222	ZnTe
73.6	0.5988	1.62	6.62	202	Te
78.8	0.6345	1.53	1.53	400	ZnTe
82	0.6557	1.48	1.48	113	Te
83.2	0.6637	1.46	1.46	210	Te

3.2. Structural characterization

X-ray diffractometer (Philips PW 1729) was employed to obtain X-ray diffractograms of $Zn_{10}Te_{90}$, $Zn_{30}Te_{70}$ and $Zn_{50}Te_{50}$ material at room temperature to get the information on their structure. These diffractograms were analysed to obtain crystallographic information on these samples. The iron target was used as a source of Fe Kα radiation with λ = 1.937355 Å. The scanning angle (2θ) was in the range of 30–85°. The X-ray diffraction pattern gives valuable information about the nature and structure of the material. The presence of sharp peaks in XRD patterns confirmed the polycrystalline nature of the material. The experimental d-values for $Zn_{10}Te_{90}$, $Zn_{30}Te_{70}$ and $Zn_{50}Te_{50}$ materials are calculated from Bragg's relation, $2d\sin\theta = n\lambda$, by taking the θ values from the peaks of XRD pattern [12]. These calculated d-values are compared with d^*-values obtained from ASTM data for ZnTe and Te. The experimental d-values of ZnTe and Te in $Zn_{10}Te_{90}$, $Zn_{30}Te_{70}$ and $Zn_{50}Te_{50}$ materials are in good agreement with the ASTM d^*-values of ZnTe and Te (Tables 1–3).

4. Results and discussion

4.1. Structural properties

Fig. 1 is the XRD patterns of $Zn_{10}Te_{90}$, $Zn_{30}Te_{70}$ and $Zn_{50}Te_{50}$ materials. From comparison among the XRD patterns it is clear that the number of peaks as well as the intensity of peaks increases with increasing Zn concentration, which indicates that the amount of

Table 3
X-ray diffraction data of $Zn_{50}Te_{50}$ material.

2θ	$\sin\theta$	d (Å)	d^* (Å)	Plane ($h\,k\,l$)	Identification
32	0.2739	3.535	3.523	111	ZnTe
35	0.2992	3.237	3.230	101	Te
37	0.3171	3.05	3.051	200	ZnTe
47	0.3987	2.429	2.427	002	Zn
48.8	0.4139	2.404	2.351	102	Te
51.6	0.4315	2.249	2.228	110	Te
53.4	0.4489	2.1579	2.159	220	ZnTe
55.4	0.4661	2.078	2.081	111	Te
57.2	0.4888	2.02	2.00	006, 105	Te
58.8	0.4907	1.981	1.980	003	Te
63.6	0.5247	1.841	1.840	311	ZnTe
66.8	0.5502	1.781	1.762	222	ZnTe
73.6	0.5797	1.615	1.616	202	Te
78.8	0.6345	1.525	1.526	400	ZnTe
82	0.6526	1.484	1.479	113	Te
86	0.6839	1.416	1.407	211	Te
87	0.6909	1.402	1.400	331	ZnTe

formation of ZnTe increases with increasing Zn concentration. There are only three peaks of ZnTe material in $Zn_{10}Te_{90}$ and remaining peaks are of Te. On the other hand in samples $Zn_{30}Te_{70}$ and $Zn_{50}Te_{50}$ there are six and seven peaks of ZnTe material, respectively, indicating that with the increasing Zn concentration the amount of formation of ZnTe increases. The formation of ZnTe is common in (1 1 1), (2 2 0) and (3 1 1) planes, but the intensity of these peaks increases in case of $Zn_{30}Te_{70}$ and $Zn_{50}Te_{50}$. The new peaks of ZnTe arise in (2 0 0), (2 2 2) and (4 0 0) planes. Thus the polycrystalline nature of material improves with the increasing concentration of Zn.

From our experimental observations, we find that $Zn_{10}Te_{90}$ material has strongest diffraction peak of ZnTe at the interplanar distance d = 1.8391 Å in (3 1 1) plane. In the same material Te has strongest peak at the interplanar distance d = 3.2229 Å in (1 0 1) plane. There are few XRD peaks of ZnTe contaminant in $Zn_{10}Te_{90}$ sample. Remaining peaks are of unreacted Te. The number of peaks of ZnTe increases in case of $Zn_{30}Te_{70}$ and $Zn_{50}Te_{50}$ materials. In $Zn_{30}Te_{70}$ and $Zn_{50}Te_{50}$ three diffraction peaks of ZnTe at the interplanar distance d = 3.5161 Å having (1 1 1) plane and d = 2.1569 Å in (2 2 0) plane and d = 1.7813 Å in (3 1 1) plane are observed, indicating the predominant growth of crystallites in these three directions. Also, Te has strongest peak at the interplanar distance d = 3.2229 Å which corresponds to (1 0 1) plane and this peak is same as in $Zn_{10}Te_{90}$ material.

In $Zn_{10}Te_{90}$ and $Zn_{30}Te_{70}$ and $Zn_{50}Te_{50}$ materials ZnTe has cubic structure, while Te has hexagonal structure. Important thing is that the formation of ZnTe increases with increasing Zn concentration. However, peaks of ZnTe which are common in the samples (i.e. $Zn_{10}Te_{90}$ and $Zn_{30}Te_{70}$ and $Zn_{50}Te_{50}$), they have become sharp and more intense with higher concentration of Zn over the peaks observed for lower Zn concentration in the sample.

4.2. Thermal properties

Simultaneous measurements of effective thermal conductivity (λ_e) and effective thermal diffusivity (χ_e) of pellets of Zn_xTe_{100-x} (x = 5, 10, 30 and 50) systems, compacted under a load of 5 tons, were carried out, at room temperature using TPS technique. Specific heat per unit volume (C_p) of the sample has been obtained using the measured values of λ_e and χ_e. Variation of λ_e, χ_e and C_p with the composition (x) of Zn has been plotted in Figs. 2–4, respectively.

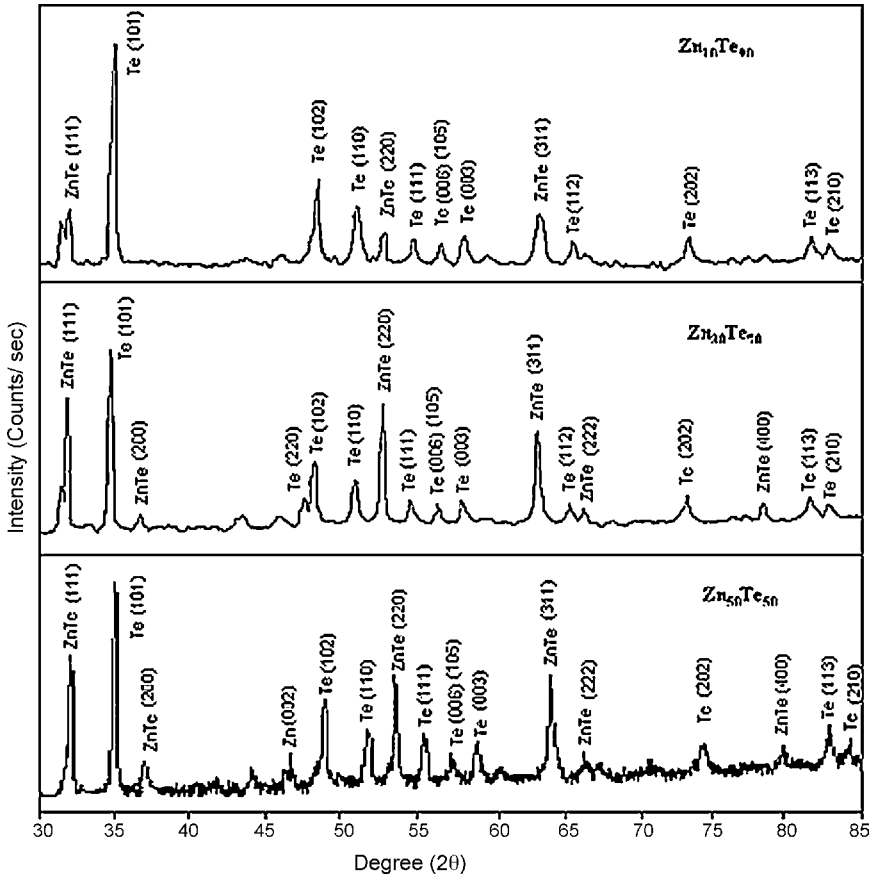

Fig. 1. X-ray diffraction patterns of $Zn_{10}Te_{90}$, $Zn_{30}Te_{70}$ and $Zn_{50}Te_{50}$ material.

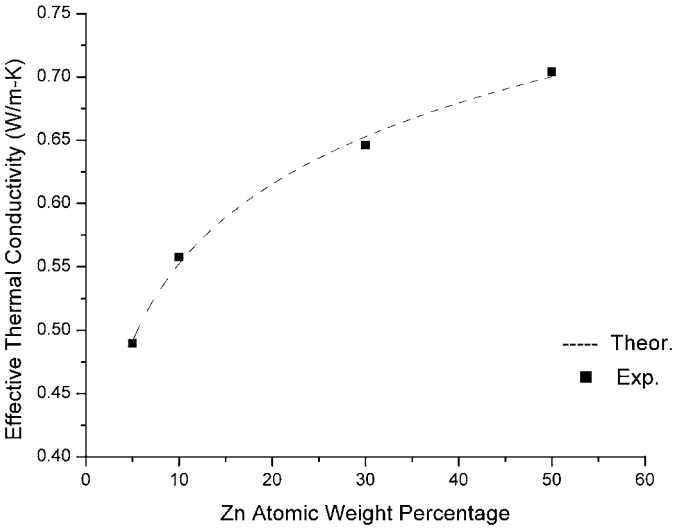

Fig. 2. Experimental and theoretical values of effective thermal conductivity.

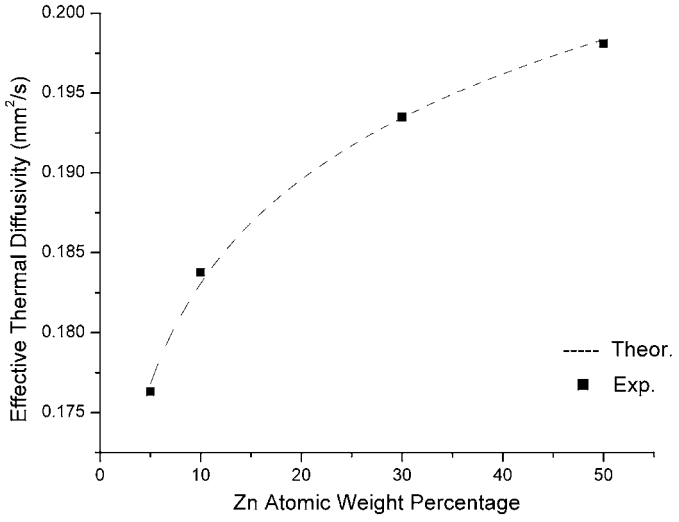

Fig. 3. Experimental and theoretical values of effective thermal diffusivity.

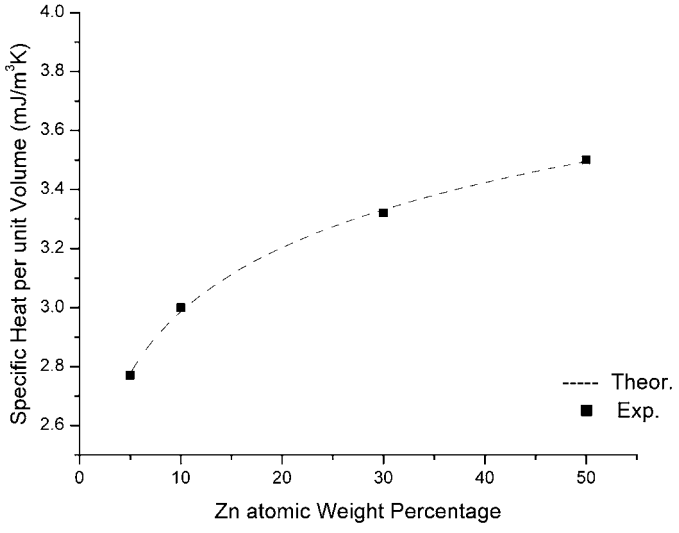

Fig. 4. Experimental and theoretical values of specific heat per unit volume.

Table 4
Value of constants 'λ_{eo}', 'χ_{eo}', 'C_{po}' and 'α', 'β', 'γ' in Eqs. (1)–(3).

$\lambda_{eo} = 0.34$ W/m K	$\alpha = 0.09$ W/m K
$\chi_{eo} = 0.16$ mm^2/s	$\beta = 0.01$ mm^2/s
$C_{po} = 2.26$ MJ/m^3 K	$\gamma = 0.33$ MJ/m^3 K

It can be observed from Figs. 2–4 that the λ_e, χ_e and C_p of materials increase in logarithmic way with increasing Zn concentration having a sharp rise at lower Zn concentration. On increasing the Zn concentration from 5 to 10, both λ_e and χ_e increases sharply. On further increase of Zn concentration in Te both λ_e and χ_e increase but this increase is not as sharp as in the beginning for lower concentration of Zn. For, Zn concentration from 30% to 50%, there is an increase in λ_e and χ_e but it is small as compared to lower concentrations of Zn.

The increase in λ_e and χ_e may be described in terms of the changing of covalent Te–Te bonds into ionic Zn–Te bonds. Zn is metallic in nature and it is found in hexagonal close packed structure. On the other hand Te, which in its stable state, exhibit semiconductor properties and have trigonal structures consisting of hexagonal arrays of helical chains of atoms with twofold coordination [13]. Although, there are fairly strong single bonds between adjacent atoms in each chain, there is evidently weak interaction of a metallic nature between the neighboring atoms of different chains. When Zn is added in lower concentration, Zn atoms make ionic bonding between chains. This in turn gives sharp increase in λ_e and χ_e, because mean free path increases due to long chain lengths. Since atomic radius of Zn is less then that of Te, therefore, Zn can easily move inside the Te chains and easily takes a proper place at suitable sites. Zn atoms serve as bridge between Te chains and form ZnTe. Due to this cross linking of Te chains via Zn atoms there occur long chains that offer long mean free path for phonons. Thus λ_e and χ_e both increases sharply at start for lower Zn concentration.

As we add more and more Zn into Te the formation of ZnTe contents increases which is also supported by XRD studies (Fig. 1). In XRD studies we see that for higher Zn concentration the sharpness of peaks increases for the case of common peaks of ZnTe. In that case the full width at half of maximum (FWHM) decreases, which is indicative of the fact that grain size increases [14] with increasing Zn concentration. Due to this increased grain size disorderness as well as porosity increases in the sample. This increase in the disorderness and porosity inturn does not allow a further increase in λ_e and χ_e and as a result λ_e, χ_e and C_p have a tendency to saturate. The overall increase in λ_e, χ_e and C_p has logarithmic nature with Zn concentration as already mentioned.

An effort has also been made to develop a relation by non-linear curve fitting of the experimental data as a function of Zn concentration. The relations established are

$$\lambda_e = \lambda_{eo} + \alpha \ln(x) \quad (1)$$

$$\chi_e = \chi_{eo} + \beta \ln(x) \quad (2)$$

$$C_p = C_{po} + \gamma \ln(x) \quad (3)$$

where 'λ_{eo}', 'χ_{eo}', 'C_{po}' and 'α', 'β', 'γ' are constants calculated through experimental conditions and 'x' is the concentration of Zn in the alloy. Values of λ_e, χ_e and C_p as obtained by these relations have been plotted in Figs. 2–4. Values obtained from the empirical

Table 5
Numerical data for verification for Eq. (4).

Concentration of Zn(x)	ln(x)	$(\lambda_e - \lambda_{eo})/\alpha$	$(\chi_e - \chi_{eo})/\beta$	$(C_p - C_{po})/\gamma$
05	1.61	1.59	1.49	1.58
10	2.30	2.35	2.36	2.36
30	3.40	3.32	3.39	3.33
50	3.91	3.96	3.88	3.96

relations are in good agreement with experimentally observed values of λ_e, χ_e and C_p. Values of constants 'λ_{eo}', 'χ_{eo}', 'C_{po}' and 'α', 'β', 'γ' for alloys are given in Table 4.

All the three above mentioned Eqs. (1)–(3) could be represented in the functional form by a single equation.

$$F(x) = A + B\ln(x)$$

$$\ln(x) = \frac{[F(x) - A]}{B}$$

Therefore, one can write

$$\ln(x) = \frac{\lambda_e - \lambda_{eo}}{\alpha} = \frac{\chi_e - \chi_{eo}}{\beta} = \frac{C_p - C_{po}}{\gamma} \quad (4)$$

This relation shows that $\ln(x)$ is a constant (Table 5) and has equal values for all three cases, i.e. effective thermal conductivity (λ_e), effective thermal diffusivity (χ_e) and specific heat per unit volume (C_p) with different constants α, β and γ.

5. Conclusions

XRD trace of the sample shows that the material is polycrystalline, in spite of the fact that the material has been prepared by melt quenching method. The enhancement in the λ_e and χ_e with the increasing concentration of Zn in Te is suggestive of the fact that a change from covalent bonding to ionic bonding takes place. The grain size of ZnTe material increases with the increasing concentration of Zn, which is responsible for the saturation of λ_e and χ_e. The experimental values of λ_e and χ_e and the values predicted by an empirical relation are of good agreement.

References

[1] A.B. Seddon, J. Non-Cryst. Solids 184 (1995) 44.
[2] M. Husain, B.P. Singh, S. Kumar, T.P. Sharma, P.J. Sebastian, Sol. Energy Mater. Sol. Cells 76 (2003) 399.
[3] K.C. Mishra, J.C. Garg, Indian J. Pure Appl. Phys. 26 (1998) 480.
[4] M. Jain, V.V. Goldvsky, J.J. Derby, J.R. Chelikowsky, Phys. Rev. B 65 (2001) 0352126.
[5] T. Mahalingam, V.S. John, G. Ravi, P.J. Sebastian, Cryst. Res. Technol. 4 (2002) 329–339.
[6] N.S. Saxena, P.R. Pradhan, G.D. Ladiwala, K. Bala, M.P. Saxena, Solid State Ionics: Mater. Appl. (1992) 723–727.
[7] K. Singh, N.S. Saxena, N.B. Maharjan, Phys. Status Solidi (a) 189 (1) (2002) 197–202.
[8] G.P. Joshi, N.S. Saxena, T.P. Sharma, V. Dixit, S.C.K. Mishra, J. Phys. Chem. Solids 64 (2003) 2391–2396.
[9] S.R. Ovshinsky, Phys. Rev. Lett. 21 (1986) 1450.
[10] S.E. Gustafsson, Rev. Sci. Instrum. 62 (1991) 797.
[11] S.E. Gustafsson, B. Suleiman, N.S. Saxena, I.U. Haq, High Temp. High Pressure 23 (1991) 289.
[12] B.D. Cullity, Elements of X-ray Diffraction, Addison-Wesley Publishing Co. Inc., Massachusetts/London, 1959.
[13] H. Ohtani, T. Yamaguchi, F. Yonezawa, Riken Rev. 29 (June) (2000).
[14] H.P. Klug, L.E. Alexander, X-ray Diffraction Procedures for Polycrystalline and Amorphous Materials, 2nd ed., John Wiley & Sons, New York, 1974.